Vol. 79: 149–164, 2017
https://doi.org/10.3354/ame01822

AQUATIC MICROBIAL ECOLOGY
Aquat Microb Ecol

Published online May 22

Modeling the effect of ultraviolet radiation on the photosynthetic potential of *Prochlorococcus* and *Synechococcus* cyanobacteria

Dailé Avila-Alonso[1,2,*], Jan M. Baetens[2], Rolando Cardenas[1], Bernard De Baets[2]

[1]Planetary Science Laboratory, Department of Physics, Universidad Central 'Marta Abreu' de Las Villas, 54830, Santa Clara, Villa Clara, Cuba

[2]KERMIT, Department of Mathematical Modelling, Statistics and Bioinformatics, Faculty of Bioscience Engineering, Ghent University, 9000 Ghent, Belgium

ABSTRACT: We used mathematical models of photosynthesis to quantify the effects of ultraviolet (UV) radiation on the photosynthetic potential of *Prochlorococcus* and *Synechococcus* marine cyanobacteria living at 0° and 40° N/S latitude. We show that UV is an environmental stressor for these organisms near the ocean surface, accounting for roughly two-thirds of the potential photosynthetic inhibition. *Prochlorococcus* showed a higher inhibition and integrated photosynthetic potential throughout the water column than *Synechococcus*, since the former is more vulnerable to UV damage at the surface and more successful at greater depths compared to the latter. The maximum photosynthetic activity was reached beneath the photoactive zone, largely due to the harmful effects of UVA. UV inhibition varies with latitude, due to variability in repair capacity for *Synechococcus*, and the existence of more diverse mechanisms of acclimation to irradiance and temperature for *Prochlorococcus*. The lowest photoinhibition is estimated to occur at 0° latitude, since the interactive effects of high temperature and irradiance have a positive effect on photoacclimation to UV damage.

KEY WORDS: Photosynthetic potential · Photosynthesis model · *Prochlorococcus* · *Synechococcus* · Ultraviolet radiation

Resale or republication not permitted without written consent of the publisher

INTRODUCTION

Solar ultraviolet (UV) radiation has been a ubiquitous physical factor throughout biological evolution on Earth (Cockell 2000, 2001), and it is known to have a wide range of harmful effects on freshwater and marine organisms (Bancroft et al. 2007, Hörtnagl et al. 2011, Llabrés et al. 2013), including phytoplankton (Vincent & Roy 1993, Cullen & Neale 1994). Numerous effects of UV on phytoplankton communities have been reported, such as the inhibition of photosynthesis, respiration and cellular motility, genetic damage, deficient nutrient uptake, and the production of toxic photoproducts, such as reactive oxygen species (ROS) (Häder 1997, Vincent & Neale 2000, Llabrés 2008). Some UV effects are due to direct photochemical reactions of UV-absorbing molecules in cells (mostly DNA, proteins, and photosystems; Häder 1997, Campbell et al. 1998, Vincent & Neale 2000, Häder et al. 2007), while other effects are indirect through the production of ROS that decrease or stop the functionality of biomolecules (such as proteins, lipids, or DNA), leading to oxidative stress (García-Pichel 1998, He & Häder 2002). Consequently, many studies have identified environmental UV radiation as an important ecological stressor that limits the production of phytoplankton and influences its growth and distribution (Holm-Hansen et al. 1993, Neale 2001).

Cyanobacteria are the most important biomass producers on Earth and play a significant role in the

*Corresponding author: davila@uclv.cu

© Inter-Research 2017 · www.int-res.com

global biogeochemical cycles of nitrogen, carbon, and oxygen (Häder et al. 2007). At present, the most abundant photosynthetic organisms on Earth are marine cyanobacteria belonging to the genera *Prochlorococcus* and *Synechococcus* (Partensky et al. 1999a), with mean ± SD global abundances of $2.9 \pm 0.1 \times 10^{27}$ and $7.0 \pm 0.3 \times 10^{26}$ cells, respectively, and realizing 25% of oceanic primary productivity (Flombaum et al. 2013). *Prochlorococcus* and *Synechococcus* account for 17–39% and 12–15% of the total global picophytoplankton biomass, respectively (Buitenhuis et al. 2012). Together, they dominate the euphotic zone of the oceanic water column, where a gradient of UV solar radiation jeopardizes surface marine life.

Prochlorococcus and *Synechococcus* are among the most important, yet enigmatic, lineages of microorganisms due to their worldwide distribution, primary productivity, and ancient evolutionary origin (Partensky et al. 1999b, Dvořák et al. 2014). One of the most striking events that occurred during the evolution of *Prochlorococcus* was the extensive genome streamlining (1.64–2.68 mega base pairs) that affected most lineages (Dufresne et al. 2005, Kettler et al. 2007, Sun & Blanchard 2014) and provided a competitive advantage to this genus (Dufresne et al. 2005) in oligotrophic areas (Partensky et al. 1999a,b). However, a small genome size implies the loss of some DNA repair genes (Dufresne et al. 2005, Partensky & Garczarek 2010, Sun & Blanchard 2014), making *Prochlorococcus* potentially more vulnerable to the effects of multiple mutations resulting from high doses of UV at the ocean surface.

Currently, the ozone layer is subject to alterations in UVB (wavelengths in the range 280–320 nm) radiation as a result of short-term changes in O_3 concentrations, not only due to natural variability, but also owing to anthropogenic activity. Moreover, high-energy photons emitted during solar bursts and storms, for instance, reach the Earth's surface as UV light of various frequencies after being scattered by the Earth's upper atmosphere, and hence might affect life at the ocean surface. It is expected that more damaging solar UVB will reach the Earth's surface as a consequence of astrophysical ionizing events in the future (on a geological timescale) (Melott & Thomas 2011).

Therefore, a quantitative assessment of the links between environmental UV and the photosynthetic potential of marine cyanobacteria is needed for greater understanding of the distribution and abundance of these organisms across the Earth's surface. The photosynthetic potential may be considered as a measure of the irradiance suitability and the photophysiological traits of photosynthetic organisms. However, the number of studies on this topic is limited. For the early periods in the evolution of cyanobacteria (i.e. the Archean eon), we refer to the contributions of Cockell (2000), Martín et al. (2012), Avila et al. (2013), and Avila-Alonso et al. (2016). For the current era, we refer to the works of Neale et al. (2014) and Neale & Thomas (2016, 2017), who used biological weighting functions (BWFs) coupled to photosynthesis–irradiance response models and determined photosynthetic parameter sets of *Prochlorococcus* and *Synechococcus*, as well as their photosynthetic rates. Taking into account the global importance of these organisms, and their different vulnerability to UV, we aimed at quantifying the effects of solar UV on the basis of their photosynthetic potential through mathematical modeling of photosynthesis.

MATERIALS AND METHODS

Model strains and study area

We modeled the photosynthetic potential of the MED4 strain of *Prochlorococcus* and the WH8102 strain of *Synechococcus*. These strains represent neither the whole physiological diversity nor the geographical and ecological distribution existing within these 2 genera, but we considered them as model strains of the *Prochlorococcus* and *Synechococcus* genera for our initial modeling attempt.

The study areas are the latitudes of 0° and 40° N/S, where the genera *Prochlorococcus* and *Synechococcus* coexist (Partensky et al. 1999a, Zwirglmaier et al. 2008). Although *Synechococcus* can be found beyond 40° N/S, the concentrations of *Prochlorococcus* decline fairly rapidly beyond this latitude (Partensky et al. 1999b, Flombaum et al. 2013), which could be considered as the biogeographical boundary of the *Prochlorococcus* distribution. The goal of this paper was to assess the photosynthetic potential under simulated *in situ* variable irradiance and temperature.

Solar radiation and oceanic radiative transfer model

We used the spectral irradiances at 0° and 40° N/S latitude for the photosynthetically active radiation (PAR, 400–700 nm) and UV radiation (280–399 nm) wavebands (Fig. 1). We assumed that the annual average PAR reaching 40° N and 40° S is similar, in agreement with the annual PAR reaching these lati-

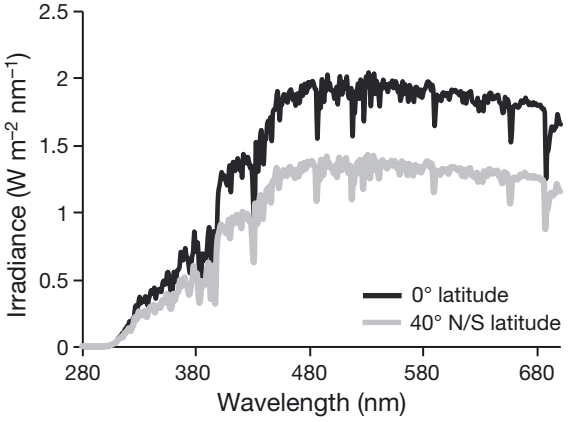

Fig. 1. UV and photosynthetically active radiation (PAR) irradiance at the ocean surface at 0° and 40° N/S latitude (ASTM G173-03(2012); www.astm.org/Standards/G173.htm)

tudes as recorded by the MODIS-Aqua sensor (http://oceancolor.gsfc.nasa.gov). For the 40° N/S latitude we used the ASTM G173-03(2012) reference spectrum for air mass 1.5 (i.e. solar zenith angle 48.2°), including the direct normal and circumsolar components for a 37° tilted surface (www.astm.org/Standards/G173.htm). This spectrum was generated by the radiative transfer code SMARTS v. 2.9.2 and is considered to be representative of cloudless conditions in the 48 contiguous US states within the period of 1 yr. Thus, we assumed this spectrum to be close to the optimum for a latitude of 40° N, as the US roughly lies between latitudes 30° and 50° N.

The above-mentioned spectrum was scaled to 0° latitude using a correction factor derived from the World Insolation Map (www.solar-facts.com/world-solar/world-insolation.php), which in turn is derived from data published by the Atmospheric Science Data Center of NASA (https://eosweb.larc.nasa.gov/cgi-bin/sse/sse.cgi). For this purpose, we divided the mean value of insolation reported for 40° N latitude by the mean reported for a latitude of 0°. The resulting correction factor (1.42) was found to hold reasonably well for the PAR band for the spectra that we obtained with the Tropospheric Ultraviolet and Visible radiative transfer model (Madronich & Flocke 1997). These spectra were obtained for the 2 equinoxes and 2 solstices (noon) and for representative locations in the Atlantic Ocean (at 0° and 40° N latitude in the same meridian: 40° W longitude). The spectra used (direct normal and circumsolar) underestimate ultraviolet irradiances. However, as illustrated by a sensitivity analysis in this paper, the results are not very sensitive to changes in the UV irradiances, so we consider this a reasonable first approach.

We considered an ocean at rest. Spectral irradiances [$E(\lambda, z)$] just below the sea surface ($z = 0^-$; see Table 1 for symbols and units), were obtained from the corresponding ones just above the sea surface ($z = 0^+$) using:

$$E(\lambda, 0^-) = (1 - R)\, E(\lambda, 0^+) \quad (1)$$

where R is the reflection coefficient obtained through the Fresnel formula (Kirk 2011) applied to the air–water interface, using a zenith angle of incidence of 0°. The spectral irradiances at depth z were calculated using Lambert-Beer's law:

$$E(\lambda, z) = E(\lambda, 0^-)\exp(-K(\lambda)\, z) \quad (2)$$

We used Jerlov's oceanic optical water type I, since its characteristics agree with the oligotrophic ocean where *Prochlorococcus* and *Synechococcus* coexist and is the most abundant type in the study area (Jerlov 1976). We used the attenuation coefficients determined by Peñate et al. (2010).

The irradiances of PAR used to estimate the photosynthetic potential of *Prochlorococcus* and *Synechococcus* were determined in agreement with Neale et al. (2014) and Neale & Thomas (2016, 2017). Those authors adjusted PAR irradiances to account for differences in the photosynthetically utilizable radiation between *in situ* and *in vitro* irradiance, through:

$$E'_{\mathrm{PAR}}(z) = E_{\mathrm{PAR}}(z)\frac{a_{\mathrm{IS}}(z)}{a_{\mathrm{PI}}} \quad (3)$$

where $a_{\mathrm{IS}}(z)$ and a_{PI} (Table 1) are calculated using Eqs. (4) and (5), respectively for a wavelength resolution $\Delta\lambda$ = 1 nm:

$$a_{\mathrm{IS}}(z) = \frac{\sum_{\lambda=400\,\mathrm{nm}}^{\lambda=700\,\mathrm{nm}} a_{\mathrm{p}}(\lambda)\, E^{Q}(\lambda, z)\, \Delta\lambda}{\sum_{\lambda=400\,\mathrm{nm}}^{\lambda=700\,\mathrm{nm}} E^{Q}(\lambda, z)\, \Delta\lambda} \quad (4)$$

$$a_{\mathrm{PI}} = \frac{\sum_{\lambda=400\,\mathrm{nm}}^{\lambda=700\,\mathrm{nm}} a_{\mathrm{p}}(\lambda)\, E^{Q}_{\mathrm{PI}}(\lambda)\, \Delta\lambda}{\sum_{\lambda=400\,\mathrm{nm}}^{\lambda=700\,\mathrm{nm}} E^{Q}_{\mathrm{PI}}(\lambda)\, \Delta\lambda} \quad (5)$$

We used *in situ* spectral irradiances in µmol m^{-2} s^{-1} nm^{-1} (Neale et al. 2014, Neale & Thomas 2016, 2017), which were determined from the ones in Fig. 1 using 4.6 µmol J^{-1} as a conversion factor (Sobrino et al. 2008).

The inhibitory effects of solar irradiance at depth z [$E^{\star}_{\mathrm{inh}}(z)$] on photosynthesis were evaluated using BWFs for the damage caused by PAR ($\varepsilon_{\mathrm{PAR}}$) and UV [$\varepsilon(\lambda)$] in Eq. (6), which were determined for the *Prochlorococcus* MED4 and *Synechococcus* WH8102 strains (Neale et al. 2014, Neale & Thomas 2017):

Table 1. Mathematical symbols and definitions; chl: chlorophyll, PAR: photosynthetically active radiation

Symbol	Definition	Units
$a_p(\lambda)$	Phytoplankton chlorophyll-specific spectral absorption coefficient	m^2 mg chl^{-1}
$a_{IS}(z)$	Irradiance weighted chlorophyll-specific absorption of PAR at depth z	m^2 mg chl^{-1}
a_{PI}	Irradiance weighted chlorophyll-specific absorption of PAR in the photoinhibitron (*in vitro*)	m^2 mg chl^{-1}
c	Scaling factor for exposures > E_{max}	–
$\varepsilon(\lambda)$	Biological weight of inhibitory effects of UV as a function of λ	m^2 mW^{-1}
ε_{PAR}	Biological weight of inhibitory effects of PAR	m^2 W^{-1}
E^{*}_{inh}	Irradiance weighted for effectiveness in inhibiting photosynthesis	–
$E(\lambda,z)$	*In situ* spectral irradiance at depth z in energy units	W m^{-2} nm^{-1}
$E^{Q}(\lambda,z)$	*In situ* spectral irradiance at depth z in quantum flux units	µmol m^{-2} s^{-1} nm^{-1}
$E^{Q}_{PI}(\lambda)$	*In vitro* spectral irradiance in quantum flux units	µmol m^{-2} s^{-1} nm^{-1}
E_{max}	Exposure that saturates repair rate	–
$E_{PAR}(z)$	Underwater PAR irradiance at depth z	W m^{-2}
$E'_{PAR}(z)$	Underwater PAR irradiance at depth z adjusted for the difference in pigment absorption of PAR *in situ* vs. *in vitro*	W m^{-2}
E_S	Characteristic irradiance for onset of saturation of photosynthesis	W m^{-2}
Inh_{UV}	Inhibition percentage due to UV damage	–
Inh_{UV+PAR}	Inhibition percentage due to combined UV and PAR damage	–
$K(\lambda)$	Attenuation coefficient for wavelength λ	m^{-1}
$P(z)$	Biomass-normalized photosynthetic rate at depth z	mg C mg chl^{-1} h^{-1}
P_S	Irradiance saturated (maximum) photosynthetic rate in the absence of inhibition	mg C mg chl^{-1} h^{-1}
$P(z)/P_S$	Photosynthetic potential at depth z	–
$(P/P_S)_T$	Integrated photosynthetic potential	–
R	Reflection coefficient of Fresnel	–

$$E^{*}_{inh}(z) = \sum_{\lambda=280\,nm}^{\lambda=399\,nm} \varepsilon(\lambda)\, E(\lambda,z)\, \Delta\lambda + \varepsilon_{PAR}\, E'_{PAR}(z) \quad (6)$$

Neale et al. (2014) and Neale & Thomas (2017) performed 4 growth treatments considering different PAR exposures and temperatures (see 'Materials and methods' in Neale et al. 2014 and Neale & Thomas 2017), i.e. high light (HL, 174 µmol m^{-2} s^{-1}) 20°C, HL 26°C, moderate light (ML, 77 µmol m^{-2} s^{-1}) 20°C, and ML 26°C. Taking into account the annual average sea surface temperature and the photosynthetically available radiation reaching the ocean surface in the concerned study area, as recorded by the MODIS-Aqua sensor (http://oceancolor.gsfc.nasa.gov), we assumed that the findings from the HL 26°C and ML 20°C treatments of Neale et al. (2014) and Neale & Thomas (2017) represent the environmental conditions for 0° and 40° N/S latitude, respectively (Table 2, Fig. 2).

Photosynthesis model

Neale et al. (2014) developed a photosynthesis model that accounts for the distinctive features of picophytoplanktonic photosynthetic responses to PAR and UV irradiance, which they then applied to *Synechococcus* and *Prochlorococcus* (Neale et al. 2014, Neale & Thomas 2016, 2017). This is the so-called E_{max} model and is characterized by the parameter E_{max} that defines the transition between light regimes where the repair increases linearly with damage ($E^{*}_{inh} \leq E_{max}$) to regimes where the repair is

Table 2. Photosynthetic parameters of *Prochlorococcus* and *Synechococcus* at 0° and 40° N/S latitude according to the treatments with high light (HL: 174 µmol m^{-2} s^{-1}) at 26°C and moderate light (ML: 77 µmol m^{-2} s^{-1}) at 20°C of Neale et al. (2014) and Neale & Thomas (2017). Parameter definitions are given in Table 1

Parameter	*Prochlorococcus*		*Synechococcus*	
	0° (HL 26°)	40° N/S (ML 20°)	0° (HL 26°)	40° N/S (ML 20°)
E_S	31.39	23.26	39.50	25.50
$\varepsilon_{PAR} \times 10^{-3}$	0.52	1.66	0.97	1.52
E_{max}	0.54	0.85	0.57	0.49

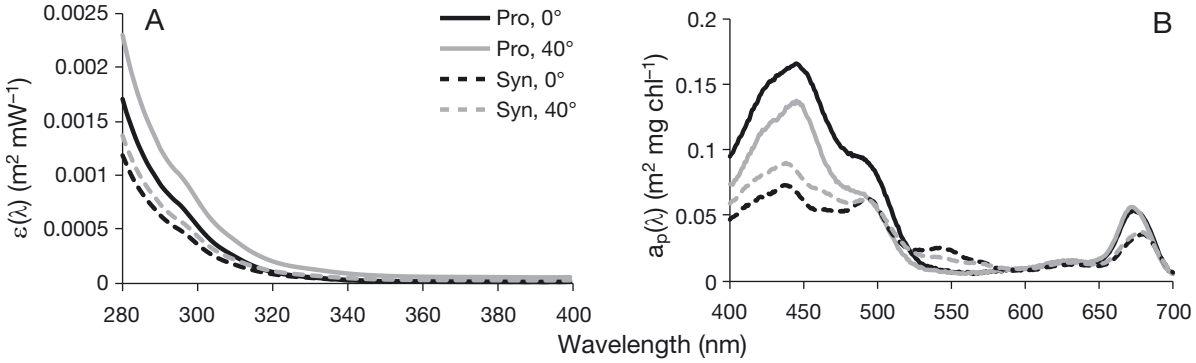

Fig. 2. (A) Biological weighting functions for UV damage and (B) chlorophyll-specific spectral absorption coefficients of *Prochlorococcus* (Pro) and *Synechococcus* (Syn) at 0° and 40° N/S latitude (Neale et al. 2014, Neale & Thomas 2017). Parameters are defined in Table 1

constant (i.e. operating at some maximum rate) ($E^*_{inh} > E_{max}$) (see Fig. 1 in Neale et al. 2014). Thus, when $E^*_{inh} \leq E_{max}$, the E model of Cullen et al. (1992a) should be used:

$$\frac{P(z)}{P_S} = \frac{1-\exp(-E'_{PAR}(z)/E_S)}{1+E^*_{inh}(z)} \quad (7)$$

otherwise the E_{max} model is valid:

$$\frac{P(z)}{P_S} = \frac{1-\exp(-E'_{PAR}(z)/E_S)}{cE^*_{inh}(z)} \quad (8)$$

where

$$c = \frac{1+E_{max}}{E_{max}} \quad (9)$$

According to Neale et al. (2014), the latter model is the most appropriate for describing the response of picophytoplankton to the full spectral irradiance, since their examination of the photosynthetic response to a weighted exposure in the laboratory revealed that the repair rate of *Synechococcus* progressively increases at a low irradiance exposure, but reaches a maximum rate above the threshold exposure defined by E_{max}. We used both the E and E_{max} models to determine the photosynthetic potential in order to compare their outputs for simulated *in situ* conditions. This is the first time that such a comparison has been made; thus, our study extends the work of Neale et al. (2014) and Neale & Thomas (2016, 2017).

The depth range for which the net photosynthetic production is positive is known as the euphotic zone. The bottom boundary of this layer is located at a depth that is reached by only 1% of the surface PAR irradiance (Kirk 2011). In clear ocean waters, this depth is about 200 m (Brenchley et al. 1998), and genera like *Prochlorococcus* and *Synechococcus* are present at high densities up to the same depth (Partensky & Garczarek 2010). Hence, assuming a maximum depth (z_{max}) of 200 m for the euphotic zone, the integrated photosynthetic potential was calculated by splitting the water column into N layers with thickness $\Delta z = 1$ m (here $N = 200$):

$$\left(\frac{P}{P_S}\right)_T = \sum_{i=1}^{N}\left(\frac{P}{P_S}\right)_i \frac{\Delta z}{z_{max}} \quad (10)$$

where $(P/P_S)_i$ is the photosynthetic potential at the bottom of the i^{th} layer of the water column. Regarding the surface layer, we determined $(P/P_S)_1$ at the surface and the bottom of this layer (i.e. 0 and 1 m, respectively).

Photobiological regimes and inhibition percentages

The inhibitory effects of UV on the photosynthetic potential of *Prochlorococcus* and *Synechococcus* were assessed by contemplating 3 photobiological regimes. A benchmark regime with the uninhibited photosynthesis (numerator of Eq. 7), a second one considering only the inhibitory effects of PAR (using only the second term in Eq. 6), and finally, a third one considering UV+PAR inhibition (Eq. 6). The latter better represents the natural photobiological regime of the concerned latitudes.

To determine the overall effect of UV+PAR inhibition on *Prochlorococcus* and *Synechococcus* photosynthesis, we considered the ratio of the integrated photosynthetic potential under UV+PAR exposure [i.e. $(P/P_S)_T$] to the integrated benchmark photosynthetic potential [i.e. $(P/P_S)_{T,\,benchmark}$]:

$$Inh_{UV+PAR} = 100\left[1-\frac{(P/P_S)_T}{(P/P_S)_{T,\,benchmark}}\right] \quad (11)$$

while the proportion of total inhibition that is due to UV was computed as:

$$Inh_{UV} = 100\left[\frac{(P/P_S)_{T,\,PAR}-(P/P_S)_T}{(P/P_S)_{T,\,benchmark}-(P/P_S)_T}\right] \quad (12)$$

Sensitivity analysis

We conducted a sensitivity analysis for the integrated photosynthetic potential under UV+PAR exposure and its inhibition percentage (Inh_{UV+PAR}) as influenced by variations in solar radiation and its penetration in the water column according to Cullen et al. (2012). We considered changes of ±10, ±15, and ±20% of the specific spectral irradiances reaching the ocean surface [$E(\lambda, 0^+)$ in Eq. 1] and the specific spectral attenuation coefficients [$K(\lambda)$ in Eq. 2]. On the other hand, taking into account that changes in sensitivity are reflected by differences in the fitted BWF coefficients, E_{max} and inhibition by PAR (ε_{PAR}) (Neale et al. 2014), we assessed the sensitivity to UV+PAR by estimating the photosynthetic potential at the Equator using the 4 BWFs and the corresponding sets of photosynthetic parameters as determined by Neale et al. (2014) and Neale & Thomas (2017) for *Synechococcus* and *Prochlorococcus*, respectively.

Alternatively, we also considered variations of the specific spectral UV irradiances reaching the ocean surface (i.e. +10, +15, +20, and +50%). The photosynthetic potentials were also determined using the global tilted irradiance (ASTM G173-03(2012)), accounting for both the direct normal and diffuse (coming from the sky and backscattered from the ground) components of solar radiation on a south-facing surface with a slope angle of 37°.

RESULTS

The plots in Fig. 3 show the photosynthetic potential versus depth for the different photobiological regimes. Given the fact that E^*_{inh} under PAR inhibition was lower than E_{max}, the entire photosynthetic profile in Fig. 3B was determined using the *E* model only. In order to compare the outputs from the *E* and E_{max} models, we considered the UV+PAR regime. The photosynthetic potential shows vertical and horizontal variability depending on the regimes, genera, and latitude. Generally speaking, PAR shows moderate inhibitory effects at the ocean surface (Fig. 3B), while UV can be a strong environmental stressor for both genera, which follows from the considerable reduction of their photosynthetic potential near the sea surface (Fig. 3C,D), although complete photoinhibition [$P(z)/P_S \approx 0$] is not reached.

UV effects in aquatic ecosystems show pronounced vertical gradients, which are reflected by the vertical spatial variability of the simulated photosynthetic potential. The most deleterious effects occur in a

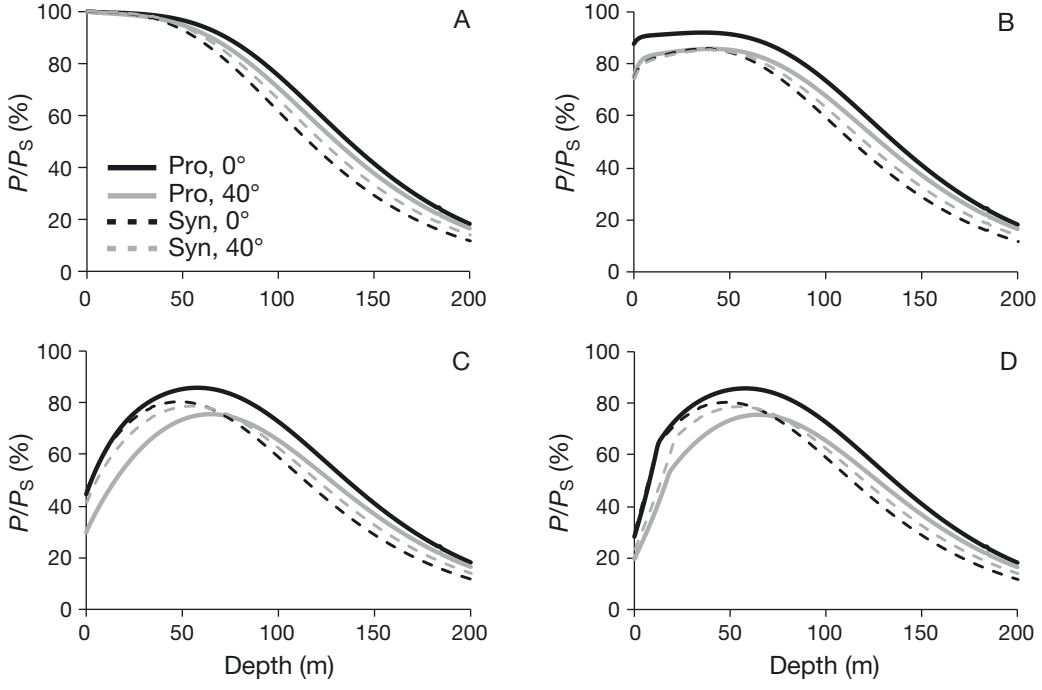

Fig. 3. Simulated photosynthetic potential profiles of *Prochlorococcus* (Pro) and *Synechococcus* (Syn) at 0° and 40° N/S latitude considering (A) uninhibited photosynthesis, (B) inhibitory effects by photosynthetically active radiation (PAR) only, and (C) inhibitory effects by UV+PAR using the *E* model and (D) inhibitory effects by UV+PAR using the E_{max} model. Parameters are defined in Table 1

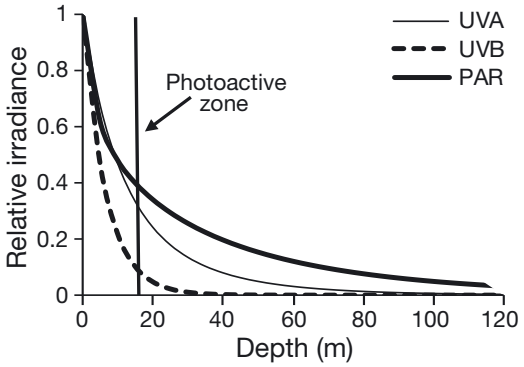

Fig. 4. Profiles of UVB, UVA (wavelength in the range 320–399 nm) and photosynthetically active radiation (PAR) as irradiance relative to the surface. The vertical line shows the lower boundary of the 'photoactive zone'

'photoactive zone' near the surface (Neale et al. 2003). This layer can be defined as the part of the water column between the water surface and the depth reached by 10% of surface-incident UVB (Neale et al. 2003). In Fig. 4, the calculated solar irradiance profiles are shown together with the lower boundary of the photoactive zone, which stretches approximately across the first 15 m of the water column. The depth reached by 10% of UVB in water type I for the UV waveband in the Central Subtropical Atlantic (integrated between 290 and 315 nm) (Piazena et al. 2002) and for the clear tropical waters of San Salvador, Bahamas (integrated between 300 and 320 nm) is approximately 13–15.5 m and 15 m, respectively (Tedetti & Sempéré 2006), which agrees with the calculated irradiance profile and the photoactive zone shown in Fig. 4. The maximum photosynthetic potential of both *Prochlorococcus* and *Synechococcus* is always reached beyond the photoactive zone, due to the propagation of the near-surface inhibition farther down into the water column.

Synechococcus attains its maximum photosynthetic potential in shallower waters than *Prochlorococcus* (Fig. 3B–D). On the other hand, deep into the water column, *Prochlorococcus* supports a higher photosynthetic potential than *Synechococcus*. Regarding horizontal variability, *Synechococcus* exhibits a similar photosynthetic potential at the concerned latitudes, irrespective of the model used, while *Prochlorococcus* shows considerable horizontal variation. The latter reaches the highest photosynthetic potential at 0° latitude, where it is similar to that of *Synechococcus* in the first 25 m of the water column. Yet, at 40°N/S latitude, it attains a lower potential than *Synechococcus* at the surface.

Prochlorococcus is more sensitive to UV damage at the Equator than *Synechococcus* is (see BWFs in Fig. 2A), although it is more resistant to PAR damage as compared to *Synechococcus* (see ε_{PAR} in Table 2, Fig. 3B), and therefore some sort of compensation allows for similar potentials in the first meters of the water column. The solar irradiances reaching the Equator are higher than those at 40°N/S latitude, while *Prochlorococcus* has a higher light absorption coefficient (Fig. 2B) and lower E_S at the Equator than *Synechococcus* (Table 2), which allows the former genus to reach a higher photosynthetic potential than the latter deep into the water column. In contrast, at 40°N/S latitude, *Prochlorococcus* shows a higher sensitivity to both UV and PAR than *Synechococcus* (Fig. 2, Table 2), while both genera have similar E_S values. This explains why we found no considerable differences between the simulated photosynthetic potential of *Prochlorococcus* and *Synechococcus* at 40°N/S latitude.

UV radiation accounts, in most cases, for the largest fraction of the integrated photosynthetic potential loss, with the highest reduction occurring at 0° latitude for *Prochlorococcus* and 40°N/S latitude for *Synechococcus* (see Inh_{UV} in Table 3). The potential of *Prochlorococcus* is more inhibited by UV+PAR and UV than that of *Synechococcus* (Table 3). Only at 0° latitude is the integrated photosynthetic potential loss (under UV+PAR exposure) of *Synechococcus* larger when evaluated over the entire water column than that of *Prochlorococcus*, due to the considerable PAR sensitivity of *Synechococcus* (high ε_{PAR}, Table 2). Consequently, *Synechococcus* displays a higher integrated photosynthetic potential in the photoactive zone than *Prochlorococcus*, while the latter has the largest photosynthetic potential when considering the entire water column (Table 3).

Although the outputs of the E_{max} model indicate higher inhibitory effects of UV than the outputs of the E model, no substantial differences were found between the photosynthetic profiles obtained using both models in the entire water column, while we found significant differences for both genera at 40° N/S latitude in the photoactive zone. The E_{max} model was applied in the first meters of the water column, where $E^{*}_{inh} > E_{max}$ (i.e. 10 and 20 m at 0° and 40°N/S latitude, respectively). The photosynthetic potentials of *Prochlorococcus* and *Synechococcus* up to 20 m at 40°N/S latitude estimated with the E model (Fig. 3C) are considerably different. In contrast, the corresponding profiles estimated with the E_{max} model are almost overlapping. The latter is due to the fact that E^{*}_{inh} is weighed by c (Eq. 9) in the E_{max} model (Eq. 8), and E_{max} is higher for *Prochlorococcus* than for *Synechococcus* (Table 2). However, the significant differ-

Table 3. Integrated photosynthetic potential and inhibition by UV+photosynthetically active radiation (PAR) and UV of *Prochlorococcus* and *Synechococcus* in the entire water column and the photoactive zone considering different latitudes (0° and 40° N/S), photobiological regimens (benchmark regime without inhibition and PAR and UV+PAR inhibition) and photosynthesis models (E and E_{max} models; see Table 1 for parameter definitions)

Regime	Integrated photosynthetic potential (%)							
	Water column				Photoactive zone			
	Prochlorococcus		*Synechococcus*		*Prochlorococcus*		*Synechococcus*	
	0°	40° N/S	0°	40° N/S	0°	40° N/S	0°	40° N/S
Without inhibition	68.87	65.88	60.27	62.90	100	100	100	100
PAR	65.96	60.29	55.20	57.49	95.74	86.16	85.18	85.04
UV+PAR (E model)	60.32	52.30	51.36	51.80	61	42.76	60.84	55.50
UV+PAR (E_{max} model)	59.66	51.19	50.81	51.03	51.82	34.02	57.48	39.85
Inhibition (%)								
Inh_{UV+PAR} (E model)	12	21	15	18	40	57	39	44
Inh_{UV} (E model)	66	59	43	51	89	75	62	66
Inh_{UV+PAR} (E_{max} model)	13	22	16	19	48	66	43	60
Inh_{UV} (E_{max} model)	68	62	46	54	91	79	65	75

ence between the outputs of the models (Fig. 3C,D) may be associated with the specific sets of photosynthetic parameters used to calculate the photosynthetic potential at 0° and 40° N/S latitude. Thus, in order to assess the influence of different photosynthetic parameters on the outputs of the models, we performed a sensitivity analysis wherein we estimated the integrated photosynthetic potential for each of 4 growth conditions for *Synechococcus* and *Prochlorococcus* determined by Neale et al. (2014) and Neale & Thomas (2017), respectively.

The sensitivity analysis involved variations in solar radiation and water transparency (Fig. 5A–D) and different sets of photosynthetic parameters (Fig. 5E,F). It shows that the largest differences between the outputs of the E and E_{max} models occur in the photoactive zone (within 22 and 20% for *Prochlorococcus* and *Synechococcus*, respectively; Fig. 5B,D,F). In contrast, the former model encloses most of the variability found by the E_{max} model for the entire water column (within 1.72 and 1.52% for *Prochlorococcus* and *Synechococcus*, respectively; Fig. 5A,C,E). The sensitivity of both models depends on the specific zone analyzed. Considering the entire water column, the outputs of the models are more sensitive to changes in the attenuation coefficients than to the solar irradiance, and vice versa for the photoactive zone. These results are in agreement with those of Cullen et al. (2012) for the entire water column. They observed a higher model sensitivity due to the variations in the chlorophyll (chl) concentration and chromophoric dissolved organic matter (CDOM) than to changes in the atmospheric ozone (see Fig. 5A–C in Cullen et al. 2012). Chl concentration and CDOM determine the optical properties of the water column (i.e. its attenuation coefficient; Kirk 2011), while atmospheric ozone affects the UV irradiance reaching the ocean surface. On the other hand, we found that both models are not very sensitive to changes in photosynthetic parameters regarding the entire water column estimates (Fig. 5E).

On the other hand, the largest differences in the photosynthetic potential due to changes in the specific spectral UV irradiances reaching the ocean surface occur in the first meters of the water column (Fig. 6). Yet, the differences between the specific integrated photosynthetic potentials across the entire water column and those considering increased UV irradiances are not higher than 3%. In agreement, the estimates made using the global tilted irradiance (i.e. direct normal and diffuse irradiances) indicate differences of about 3 to 4% for the E and E_{max} models, respectively, which suggests that these models are not very sensitive to changes in UV irradiances.

DISCUSSION

Model validation

This work constitutes a modeling study of the effects of UV radiation on the photosynthetic potential of *Prochlorococcus* and *Synechococcus*, which is an extension of the works by Neale et al. (2014) and Neale & Thomas (2017). In order to assess the validity of our simulation results, a comparison with *in situ* profiles of *Prochlorococcus* and *Synechococcus* primary production (accounting for UV damage) is

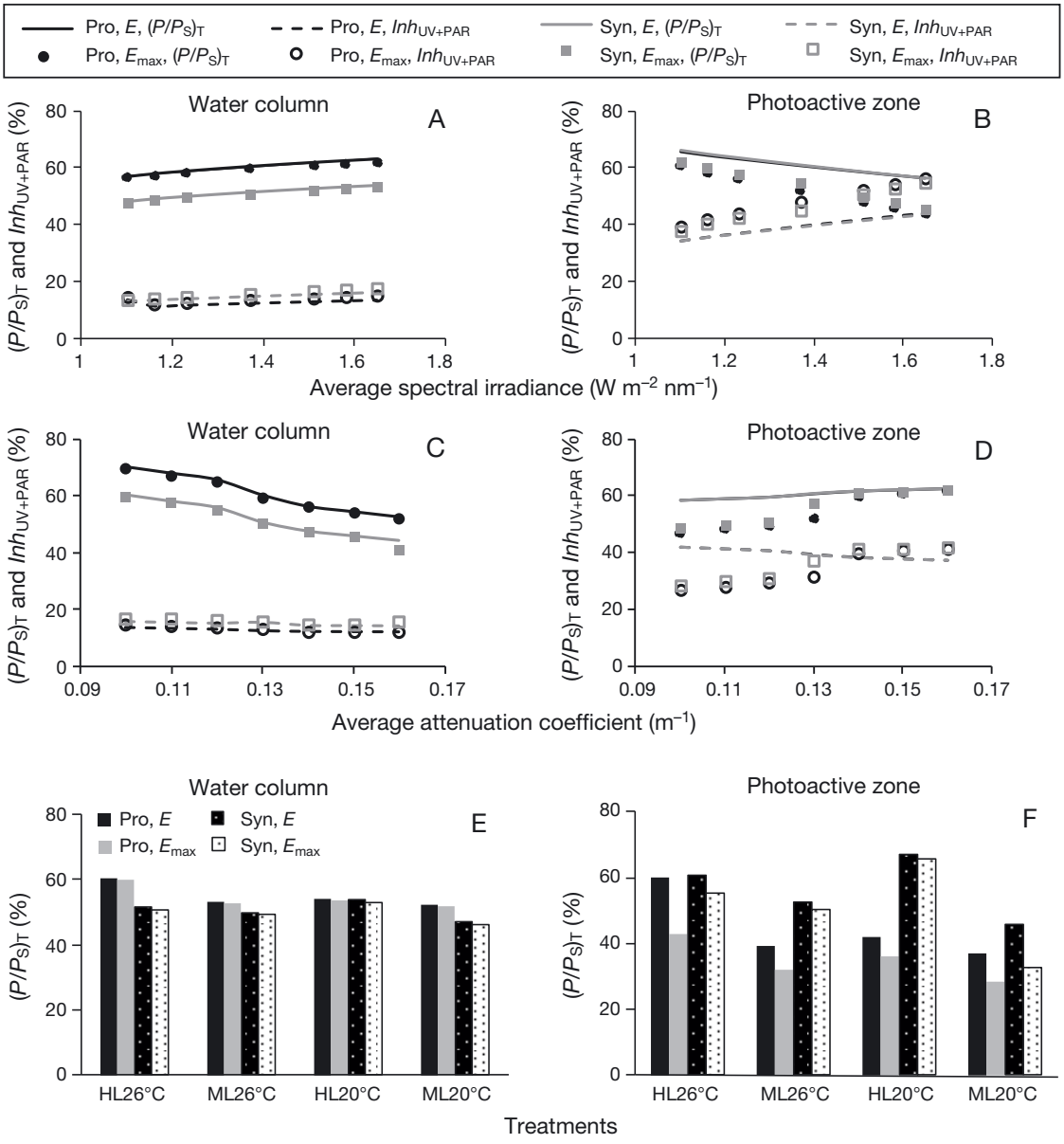

Fig. 5. Sensitivity analysis of the E and E_{max} models for the integrated photosynthetic potential and percent inhibition of *Prochlorococcus* (Pro) and *Synechococcus* (Syn) by UV+photosynthetically active radiation (PAR) in the water column and the photoactive zone, as a function of (A,B) solar radiation reaching the ocean surface; (C,D) attenuation coefficient. The reference is the equatorial latitude, with an average irradiance reaching the ocean surface of 1.37 W m^{-2} nm^{-1}, an average attenuation coefficient of 0.13 m^{-1}, and a biological weighting function (BWF) of high light (HL) at 26°C. (E,F) Photosynthetic potential for the reference considering different sets of photosynthetic parameters. Parameters are defined in Table 1; ML: moderate light

needed. Neale et al. (2014) and Neale & Thomas (2017) performed the first estimations of the primary production loss by UV radiation in these genera, but they stated that there are few other reports to which these estimates can be compared. Moreover, the available P vs. E curves are determined only as a function of PAR irradiance, so more measurements of primary productivity under UV exposure are needed (Neale & Thomas 2017).

The higher estimated photosynthetic potential of *Prochlorococcus* at 0° than at 40° N/S latitude and the similar photosynthetic potential of *Synechococcus* at those latitudes (Fig. 3C,D) agree with the estimations of present global biogeographic patterns of these genera at the sea surface. *Prochlorococcus* is the most abundant in the equatorial region, decreasing toward 40° N/S latitude, while *Synechococcus* is equally abundant across the entire latitudinal band between

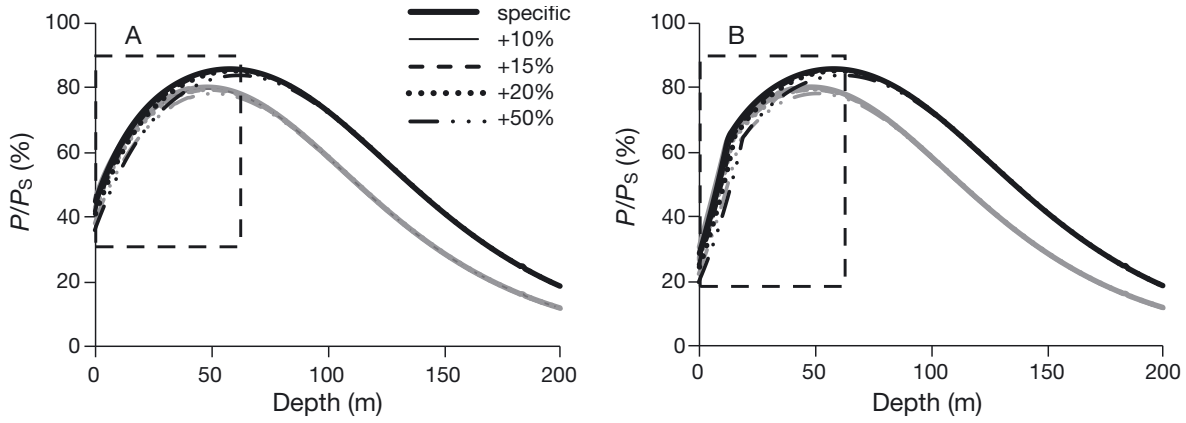

Fig. 6. Simulated photosynthetic potential profiles of *Prochlorococcus* (black) and *Synechococcus* (gray) at 0° latitude considering changes of +10, +15, +20, and +50% of the specific spectral UV irradiances reaching the ocean surface using the (A) E and (B) E_{max} models. Note that some profiles overlap, obscuring the curves. Specific profiles refer to the estimated reference profiles in Fig. 3C,D. Dashed rectangles show the variations in the upper water column. Parameters are defined in Table 1

40° N and 40° S (Flombaum et al. 2013). In agreement, Hartmann et al. (2014) reported similar horizontal patterns for *Prochlorococcus* and *Synechococcus* in the Atlantic ocean between 30° N and 30° S on the basis of their cell-specific CO_2 fixation rates.

The simulated vertical profiles of the photosynthetic potential account for the UV sensitivity and efficient absorption and use of PAR of *Prochlorococcus* and *Synechococcus.* Dishon et al. (2012) used similar photophysiological traits to describe the vertical distribution of those genera on the basis of their biomass in the Mediterranean and Red Seas. They reported that *Synechococcus* and *Prochlorococcus* generally dominate the upper and deeper optical habitats of the water column, respectively, and this pattern is reflected by our simulated photosynthetic potential profiles. However, this agreement between the photosynthetic potential and biomass merely serves as a motivation for a more extensive future analysis of the correspondence between those variables.

The benchmark photosynthetic potential profiles shown in Fig. 3A agree with the ones reported by Neale et al. (2014) and Neale & Thomas (2017). The former determined the potential productivity on the basis of the average response of the *Synechococcus* WH8102 and WH7803 strains (ML 20°C). They reported that photosynthesis is light saturated down to a depth of about 23 m due to PAR attenuation at this depth, while the uninhibited profile for *Synechococcus* WH8102 (40° N/S latitude, ML 20°C) is light saturated down to 25 m (Fig. 3A). The average depth at which the simulated uninhibited photosynthesis of *Prochlorococcus* at 25° N drops (i.e. 1% below P_S) is 44 m (range 28–57 m, considering monthly variations; Neale & Thomas 2017). This agrees with our results shown in Fig. 3A, as we found that this occurs at 41 and 35 m at 0° and 40° N/S latitude, respectively.

The maximum photosynthesis rate of *Synechococcus* WH8102 for HL 26°C and ML 20°C in Neale et al. (2014) under UV+PAR inhibition is reached approximately at a depth of 44 and 55 m, respectively, while we found that the maximum photosynthetic potential is attained at 48 and 55 m at 0° and 40° N/S latitude, respectively (Fig. 3C,D). However, for *Prochlorococcus*, Neale & Thomas (2017) reported that the maximum rates occur at a shallower depth than we found (Fig. 3C,D). This may be attributed to a difference between the attenuation coefficients and irradiance datasets used in our study and that of Neale & Thomas (2017), as well as to their procedure to adjust $E^{\star}_{inh}$ to the sea surface temperature between 20 and 26°C.

The photosynthesis rate normalized with respect to the chl *a* concentration is not a reliable proxy for the relative growth rate of phytoplankton (Cullen et al. 1992b). However, Vaulot et al. (1995) reported that both the photosynthetic assimilation ratio and growth rate of *Prochlorococcus* in the equatorial Pacific are reduced near the surface. In agreement, the specific growth rate of phytoplankton species has been calculated considering a proportional relationship with the photosynthesis rate normalized with respect to the chl *a* concentration (Cullen et al. 1992b, Laws 2013) or the maximum (light saturated) photosynthetic rate (Hickman et al. 2010). The maximum (light saturated) photosynthetic rate depends on the maximum possible growth rate (Hickman et al. 2010). Hence, we may compare our simulated profiles with field and laboratory observations by assuming a proportional relationship between those variables.

Liu et al. (1997) reported that the maximum estimated growth rate of *Prochlorococcus* in the equatorial Pacific occurs at depths ranging from 40 to 70 m. According to our simulations, the highest *Prochlorococcus* photosynthetic potential (i.e. 86%) at the Equator is attained at 60 m (Fig. 3C,D). *Prochlorococcus* strains dominating the surface waters have an irradiance optimum for photosynthesis of approximately 200 µmol m^{-2} s^{-1} (Hess et al. 2001), which is confirmed by the study of Moore & Chisholm (1999). This PAR irradiance is reached at 68 and 55 m at 0° and 40° N/S latitude, respectively, according to the simulated radiative propagation in the water column (results not shown), where this genus shows a high photosynthetic potential (Fig. 3C,D). Liu et al. (1998) found that *Synechococcus* grows much faster than *Prochlorococcus* in the upper water column, and reaches its maximum growth rate at shallower depths than *Prochlorococcus*. Six et al. (2004) determined that the maximum growth rate of *Synechococcus* WH8102 occurs at an irradiance of 207 µmol m^{-2} s^{-1}, which is reached at 50 m in our study (averaged over 0° and 40° N/S latitude), where a high photosynthetic potential for *Synechococcus* was estimated (Fig. 3C,D).

On the other hand, Neale & Thomas (2017) reported that the production of *Prochlorococcus* and *Synechococcus* in the central Pacific and the eastern Pacific Ocean near the Equator was reduced by 7–28% and 7–73% under UV+PAR exposure in the euphotic zone and the surface mixed layer, respectively, depending on the strain and *in situ* conditions. For the UV+PAR photobiological regime, we estimated that the photosynthetic potential over the entire water column, depending on genus and latitudes, was reduced by 12–21% and 13–22% using the E and E_{max} models, respectively. Considering only the photoactive zone, production was reduced by 39–57% and 43–66%, using the above models. Furthermore, Neale & Thomas (2017) reported that UV accounts for two-thirds of the productivity reduction in the study area, which in general agrees with our results (Table 3).

Inhibition and mechanisms to cope with photodamage

The higher photosynthetic loss of *Prochlorococcus* and *Synechococcus* due to the combined inhibitory effects of UV and PAR compared to the individual effects of UV and PAR (Table 3) has been reported previously. The total and slow-relaxing, non-photochemical quenching in *Prochlorococcus* MED4 is significantly higher during exposure to UV+PAR compared to that of PAR alone (see Fig. 1 in Kulk et al. 2013). In contrast, fast-relaxing, non-photochemical quenching decreases significantly during exposure to UV, which suggests an inhibitory effect of this waveband to the reaction center of PSII (Kulk et al. 2013). In agreement, Fragoso et al. (2014) determined that the loss of photosynthetic activity in *Synechococcus* WH8102 was significantly faster when cells were exposed to a moderate UV+PAR treatment than to UV or PAR separately. UV+PAR affects more targets in cyanobacteria than UV or PAR alone, including both the D1 and D2 protein subunits of the PSII reaction center and other independent targets of the PSII complex (reviewed by Fragoso et al. 2014).

The fact that the maximum photosynthetic potential of *Prochlorococcus* and *Synechococcus* occurs beyond the photoactive zone (Figs. 3C,D & 4) could indicate the deleterious effects of UVA on these organisms. This spectral range, although it is less harmful because it is less energetic than UVB, is also an inhibitor of photosynthesis at natural doses. Although UVB is more damaging on a per photon basis (Buma et al. 2001), most inhibition of primary production and degradation of photosynthetic pigments can be caused by the much larger flux of UVA (Neale 2000, Conan et al. 2008). Radiation at these wavelengths can penetrate several meters into the water column, affecting phytoplanktonic organisms over greater depths than UVB (Fig. 4). Sommaruga et al. (2005) determined that UVA radiation was effective in reducing the cell-specific chlorophyll fluorescence of *Prochlorococcus* only.

The lower UV+PAR inhibition of *Synechococcus* and its higher integrated photosynthetic potential in the photoactive zone as compared to *Prochlorococcus* (Table 3) are consistent with field reports, and are probably caused by the fact that *Synechococcus* is better adapted than *Prochlorococcus* for growing and photosynthesizing near the water surface, where UV irradiance is higher. The former genus has developed efficient ways to cope with UV stress (Campbell et al. 1998, Mella-Flores et al. 2012), although some of its structures (like phycobilisomes) are vulnerable to UVB damage (Sah et al. 1998, Six et al. 2007a).

It has been suggested that a part of the *Synechococcus* WH8102 photoadaptation strategy to cope with photodamage lies in increasing its repair capacity due to the large changes in E_{max} as compared with its BWF coefficients under different growth conditions (Neale et al. 2014). Specifically, E_{max} increases with high irradiance and temperature, allowing this strain to increase its repair capacity, and conse-

quently reach a higher photosynthetic potential in the photoactive zone at 0° latitude than at 40° N/S.

Fragoso et al. (2014) determined that *Synechococcus* WH8102 increases its repair capacity over shorter timescales (minutes–hours) in response to acute UV exposure, which could be related to increased expression of a more UV-resistant isoform of the PSII reaction center core protein, D1 (i.e. D1:1 and D1:2 isoforms). In agreement, Murphy et al. (2017) showed that the PSII repair mechanism always appears as a metabolically viable strategy for *Synechococcus* to counteract PSII photoinactivation under visible light. Mackey et al. (2013) found that for *Synechococcus* WH8102, growth at higher temperatures led to an increase in the abundance of photosynthetic complexes (e.g. phycobilisome pigment proteins, subunits of PSII, PSI, cytochrome b6f), which allows for an increase in photosynthetic electron flux to meet the metabolic requirement during rapid growth, avoiding damage.

On the other hand, *Prochlorococcus* shows a high variability of its BWF coefficients (Fig. 2A) with the lowest values at high irradiance and temperature exposure (at 0° latitude, HL 26°C). However, in contrast to *Synechococcus* WH8102, for *Prochlorococcus* E_{max} decreases with higher irradiance and increased temperature (see Table 1 in Neale & Thomas 2017), which can be regarded as an augmented sensitivity. Nevertheless, given that a lower E_{max} implies a lower BWF, it could be thought that *Prochlorococcus* has diverse photoprotective mechanisms of acclimation to irradiance and temperature beyond normal repair mechanisms. Taking into account that UV-induced repair is more important for *Synechococcus* than *Prochlorococcus* (~2-fold vs. ~5-fold at noon, respectively), the latter genus seemingly survives the stressful hours of the day by relying on a minimal set of protection mechanisms and by temporarily bringing down several key metabolic processes (Mella-Flores et al. 2012).

In *Prochlorococcus*, very few genes coding for protective systems are maximally expressed under high UV+PAR exposures. For instance, the *ptox* gene encoding for plastoquinol terminal oxidase (PTOX), an alternate electron transfer pathway that acts as a sink for a significant fraction of the photosynthetic electron transport under high irradiance (Bailey et al. 2008, Mackey et al. 2008), is highly expressed in *Prochlorococcus* (Mella-Flores et al. 2012). The expression of the *ptox* gene may play a key role in the phototolerance of *Prochlorococcus* MED4 (Berg et al. 2011). *Prochlorococcus* has a selective advantage with respect to oxidative damage from the high radiation intensity (UV+PAR), since it evolved in the presence of a heterotrophic microbial community that reduces the concentrations of toxic ROS (Morris et al. 2011), but still it is more sensitive than *Synechococcus.*

The lower inhibition of *Prochlorococcus* at 0° (HL 26°C) than at 40° N/S latitude (ML 20°C; Table 3) agrees with laboratory findings on the basis of its physiological response to the high irradiance and temperature. Kulk et al. (2013) reported that temperature acclimation influences the relative contribution of photoinhibition and photoprotective mechanisms of *Prochlorococcus* MED4 in response to high irradiance exposure. More precisely, the changes in its photophysiology (e.g. increased light harvesting, increased electron transport, and reduced photoinhibition) at high temperature possibly allow for photosynthesis at higher irradiance intensities (Kulk et al. 2012).

Photosynthesis deep in the water column

Similar to other approaches, we assumed uniform physiological parameters across the entire water column, since the photosynthetic parameters were not corrected for decreases in temperature and irradiance deep in the water column. Nevertheless, although the simulated deep photosynthetic potential provides a conservative result, its analysis is useful to compare the overall responses implicit in the models (Neale et al. 2014).

Despite the higher UV inhibition of *Prochlorococcus* compared to *Synechococcus,* the former has a higher integrated photosynthetic potential across the entire water column (Table 3) because of its capability to support photosynthesis deep in the water column, which agrees with the findings of Liu et al. (1995) and Rii et al. (2016) considering the integrated primary production for *Prochlorococcus* and *Synechococcus* assemblages. Rii et al. (2016) observed that *Prochlorococcus* increases its primary production up to great depths in the euphotic zone in the southeastern Pacific Ocean. This genus contributes 10% of the total ^{14}C assimilated by the whole photosynthetic marine community at 175 m depth at Station ALOHA (Björkman et al. 2015).

The fact that the simulated photosynthetic potential of *Prochlorococcus* remains higher at depths greater than 50 m compared to that of *Synechococcus* (Fig. 3) was also determined by Shimada et al. (1996). *Synechococcus* is generally restricted to surface water habitats because of its spectral require-

ments. Indeed, the absorption spectrum of *Synechococcus* is characterized by an absorption peak at 550–560 nm (Ting et al. 2002) (Fig. 2B). This green-light-harvesting capability gives *Synechococcus* an advantage close to the surface, where green light is still abundant (Ting et al. 2002, Dishon et al. 2012). However, *Synechococcus* WH8102 also has a high light absorption in the blue region due to its high phycourobilin:phycoerythrobilin ratio (Six et al. 2007b).

On the other hand, the acquisition of divinyl chlorophylls was an important evolutionary milestone for the genus *Prochlorococcus* in order to avoid the intense irradiance flux near the water surface (Ting et al. 2002, Ito & Tanaka 2011), as it allows these organisms to photosynthesize and grow at great depths (even beneath the euphotic zone; Dishon et al. 2012), where blue light predominates. The higher photosynthetic potential of *Prochlorococcus* deeper in the water column (Fig. 3) can mainly be explained by the higher light absorption efficiency due to its small size (Morel et al. 1993), and the more efficient use of the absorbed light by this genus as compared to *Synechococcus* (see values of E_S in Table 2). Shimada et al. (1996) reported that the photosynthetic quantum yield of *Prochlorococcus* is higher than that of *Synechococcus* at any wavelength between 400 and 700 nm and that the photosynthetic activity of *Prochlorococcus* is higher than that of *Synechococcus* in the blue-light-rich environment of the oceanic euphotic zone.

The estimated photosynthetic potentials at 200 m are approximately one-third of those at the surface. The former could follow from the low attenuation coefficients in the blue spectrum used in this paper, allowing for a high penetration of PAR irradiances up to 200 m. The attenuation coefficient at 490 nm used here approximates the minimum enclosed in the complete mission data of several remote sensors (http://oceancolor.gsfc.nasa.gov), so it could be considered that our results are representative of the clearest ocean waters in the study area.

Sensitivity analysis

The fact that both the E and E_{max} models are more sensitive to changes in the attenuation coefficient in the entire water column than in the photoactive zone is caused by changes in the light fluxes up to greater depths in the former. The photosynthetic potential of *Prochlorococcus* and *Synechococcus* considering changes of ±10, ±15, and ±20% of the attenuation coefficients remains practically constant across the first 60 and 50 m of the water column (results not shown). Only beyond these depths are considerable differences observed. These results agree with those of Peñate et al. (2014) for changes of ±10% of the attenuation coefficients in oceanic water type I. We therefore conclude that the simulated near-surface inhibition is not affected by changes in the attenuation coefficients.

Neale et al. (2014) calculated the biomass-specific productivity profiles of *Synechococcus* WH8102 and WH7803 using photosynthetic parameter sets (including BWFs) for different growth conditions. They reported that the average biomass-specific productivity varies by a factor of 3 among the considered parameter sets. The simulated responses were less variable for WH8102 than for WH7803, and the magnitude of the change was mainly determined by the magnitude of the change of the irradiance saturated (maximum) photosynthetic rate in the absence of inhibition (i.e. P_S in Eqs. 7 and 8) with growth temperature. Thus, it could be argued that different values of the photosynthetic potential should not affect the global estimates of the photosynthetic rate, irrespective of the moderate sensitivity of the E and E_{max} models to the photosynthetic parameter variation (Fig. 5E,F).

According to the relatively good agreement between the results obtained using the E and E_{max} models in this work (Figs. 3 & 5, Table 3), we conclude that both models can be used to assess the integrated primary productivity of *Prochlorococcus* and *Synechococcus* in the entire photic zone of the water column. The differences we found between the E and E_{max} models are smaller than those reported by Cullen et al. (2012) comparing their depth-integrated model (DIM) of primary production and numerical models (6%). Those authors concluded that both models lead essentially to the same results, so DIM is suitable for examining patterns in global ocean productivity.

In contrast, taking into account the large differences between the simulated integrated photosynthetic potential in the photoactive zone using the E and E_{max} models, the latter appears to be more suitable to calculate the integrated primary production in surface layers of oceans where the irradiance fluxes penetrating the water column are too high (e.g. photoactive zone, shallow mixed layer, etc.). Neale et al. (2014) reported that the E_{max} model gives a better agreement between the observed and calculated biomass-specific photosynthesis of *Synechococcus* at a high UV+PAR exposure (i.e. $E^{\star}_{inh} > E_{max}$,

which occurs in the surface layer of the ocean) than the E model. The latter tends to overestimate photosynthesis under these conditions, but shows a good agreement at low exposure (i.e. $E^{*}_{inh} \leq E_{max}$).

CONCLUSIONS

We found that UV radiation is responsible for approximately two-thirds of the reduction in the photosynthetic potential of the 2 investigated genera. *Synechococcus* shows a higher integrated photosynthetic potential in the photoactive zone than *Prochlorococcus*, while the maximum photosynthetic activity of these genera occurs below the photoactive zone, indicating the inhibitory effects of the UVA waveband. Generally speaking, *Prochlorococcus* shows a higher inhibition and integrated productivity across the entire water column than *Synechococcus*, since it is more vulnerable to UV damage at the surface and more successful at greater depths. In general, UV inhibition varies with latitude for *Prochlorococcus* and *Synechococcus*, as a consequence of variations in the repair capacity for *Synechococcus*, and more diverse mechanisms of acclimation to irradiance and temperature for *Prochlorococcus*. The photosynthetic potential was more reduced due to the combined inhibitory effects of UV and PAR at 40° N/S latitude, since the interactive effects of high temperature and irradiance at the Equator apparently have a positive result on photoacclimation to UV damage. Thus, the highest integrated photosynthetic potentials were mainly reported at 0° latitude. The E and E_{max} models can be used to calculate the integrated primary productivity of *Prochlorococcus* and *Synechococcus* in the photic zone of the water column, while the E_{max} model is more suitable for assessing the integrated primary productivity in the surface layers of the ocean.

Acknowledgements. We thank Dr. Patrick Neale and his colleagues for kindly permitting us to use data from their most recent papers on *Prochlorococcus* and *Synechococcus* and Dr. Osmel Martin for help with acquiring irradiance data. We also thank the anonymous reviewers for their valuable suggestions on earlier versions of this manuscript. This work was supported by the Special Research Fund (BOF) of Ghent University, Belgium, Grant Code 01W03715.

LITERATURE CITED

Avila D, Cardenas R, Martin O (2013) On the photosynthetic potential in the very Early Archean oceans. Orig Life Evol Biosph 43:67–75

Avila-Alonso D, Baetens JM, Cardenas R, De Baets B (2016) Assessing the effects of ultraviolet radiation on the photosynthetic potential in Archean marine environments. Int J Astrobiol, doi:10.1017/S147355041600032X

Bailey S, Melis A, Mackey KR, Cardol P and others (2008) Alternative photosynthetic electron flow to oxygen. Biochim Biophys Acta 1777:269–276

Bancroft BA, Nick J, Blaustein AR (2007) Effects of UVB radiation on marine and freshwater organisms: a synthesis through meta-analysis. Ecol Lett 10:332–345

Berg GM, Shrager J, van Dijken G, Mills MM, Arrigo KR, Grossman AR (2011) Responses of *psbA*, *hli* and *ptox* genes to changes in irradiance in marine *Synechococcus* and *Prochlorococcus.* Aquat Microb Ecol 65:1–14

Björkman KM, Church MJ, Doggett JK, Karl DM (2015) Differential assimilation of inorganic carbon and leucine by *Prochlorococcus* in the oligotrophic North Pacific subtropical gyre. Front Microbiol 6:1401

Brenchley PJ, Brenchley P, Harper D (1998) Palaeoecology: ecosystems, environments and evolution. Chapman & Hall, London

Buitenhuis E, Li W, Vaulot D, Lomas M and others (2012) Picophytoplankton biomass distribution in the global ocean. Earth Syst Sci Data Discuss 5:221–242

Buma AGJ, Helbling EW, de Boer MK, Villafañe VE (2001) DNA damage patterns in temperate South-Atlantic picophytoplankton assemblages exposed to solar ultraviolet radiation. J Photochem Photobiol B 62:9–18

Campbell D, Eriksson MJ, Oquist G, Gustafsson P, Clarke AK (1998) The cyanobacterium *Synechococcus* resists UV-B by exchanging photosystem II reaction-center D1 proteins. Proc Natl Acad Sci USA 95:364–369

Cockell CS (2000) Ultraviolet radiation and the photobiology of Earth's early oceans. Orig Life Evol Biosph 30:467–499

Cockell CS (2001) A photobiological history of Earth. In: Cockell CS, Blaustein AR (ed) Ecosystems, evolution, and ultraviolet radiation. Science+Bu, New York, NY, p 1–36

Conan P, Joux F, Torréton JP, Pujo-Pay M, Douki T, Rochelle-Newall E, Mari X (2008) Effect of solar ultraviolet radiation on bacterio- and phytoplankton activity in a large coral reef lagoon (southwest New Caledonia). Aquat Microb Ecol 52:83–98

Cullen JJ, Neale PJ (1994) Ultraviolet radiation, ozone depletion and marine photosynthesis. Photosynth Res 39: 303–320

Cullen JJ, Neale PJ, Lesser MP (1992a) Biological weighting function for inhibition of phytoplankton photosynthesis by ultraviolet radiation. Science 258:646–650

Cullen JJ, Yang X, MacIntyre HL (1992b) Nutrient limitation of marine photosynthesis. In: Falkowski PG, Woodhead AD (eds) Primary productivity and biogeochemical cycles in the sea. Springer Science+Business Media, New York, NY, p 69–88

Cullen JJ, Davis RF, Huot Y (2012) Spectral model of depth-integrated water column photosynthesis and its inhibition by ultraviolet radiation. Global Biogeochem Cycles 26:GB1011

Dishon G, Dubinsky Z, Caras T, Rahav E, Bar-Zeev E, Tzubery Y, Iluz D (2012) Optical habitats of ultraphytoplankton groups in the Gulf of Eilat (Aqaba), Northern Red Sea. Int J Remote Sens 33:2683–2705

Dufresne A, Garczarek L, Partensky F (2005) Accelerated evolution associated with genome reduction in a free-living prokaryote. Genome Biol 6:R14

Dvořák P, Casamatta DA, Paulíčková A, Hašler P, Ondřej V, Sanges R (2014) *Synechococcus*: 3 billion years of global dominance. Mol Ecol 23:5538–5551

Flombaum P, Gallegos JL, Gordillo RA, Rincón J and others (2013) Present and future global distributions of the marine cyanobacteria *Prochlorococcus* and *Synechococcus.* Proc Natl Acad Sci USA 110:9824–9829

Fragoso GM, Neale PJ, Kana TM, Pritchard AL (2014) Kinetics of photosynthetic response to ultraviolet and photosynthetically active radiation in *Synechococcus* WH8102 (Cyanobacteria). Photochem Photobiol 90:522–532

García-Pichel F (1998) Solar ultraviolet and the evolutionary history of cyanobacteria. Orig Life Evol Biosph 28:321–347

Häder DP (1997) Penetration and effects of solar UV-B on phytoplankton and macroalgae. Plant Ecol 128:5–13

Häder DP, Kumar HD, Smith RC, Worrest RC (2007) Effects of solar UV radiation on aquatic ecosystems and interactions with climate change. Photochem Photobiol Sci 6: 267–285

Hartmann M, Gomez-Pereira P, Grob C, Ostrowski M, Scanlan DJ, Zubkov MV (2014) Efficient CO_2 fixation by surface *Prochlorococcus* in the Atlantic Ocean. ISME J 8: 2280–2289

He YY, Häder DP (2002) Reactive oxygen species and UV-B: effect on cyanobacteria. Photochem Photobiol Sci 1: 729–736

Hess WR, Rocap G, Ting CS, Larimer F, Stilwagen S, Lamerdin J, Chisholm SW (2001) The photosynthetic apparatus of *Prochlorococcus*: insights through comparative genomics. Photosynth Res 70:53–71

Hickman AE, Dutkiewicz S, Williams RG, Follows MJ (2010) Modelling the effects of chromatic adaptation on phytoplankton community structure in the oligotrophic ocean. Mar Ecol Prog Ser 406:1–17

Holm-Hansen O, Lubin D, Helbing E (1993) Ultraviolet radiation and its effects on organisms in aquatic environments. In: Young A, Björn L, Moan J, Nultsch W (ed) Environmental UV photobiology. Plenum Press, New York, NY, p 379–425

Hörtnagl P, Pérez M, Sommaruga R (2011) Contrasting effects of ultraviolet radiation on the growth efficiency of freshwater bacteria. Aquat Ecol 45:125–136

Ito H, Tanaka A (2011) Evolution of a divinyl chlorophyll-based photosystem in *Prochlorococcus.* Proc Natl Acad Sci USA 108:18014–18019

Jerlov NG (1976) Marine optics. Elsevier Scientific Publishing Company, Amsterdam

Kettler GC, Martiny AC, Huang K, Zucker J and others (2007) Patterns and implications of gene gain and loss in the evolution of *Prochlorococcus.* PLOS Genet 3:e231

Kirk JTO (2011) Light and photosynthesis in aquatic ecosystems, 3rd edn. Cambridge University Press, New York, NY

Kulk G, de Vries P, van de Poll WH, Visser RJW, Buma AGJ (2012) Temperature-dependent growth and photophysiology of prokaryotic and eukaryotic oceanic picophytoplankton. Mar Ecol Prog Ser 466:43–55

Kulk G, de Vries P, van de Poll WH, Visser RJW, Buma AGJ (2013) Temperature-dependent photoregulation in oceanic picophytoplankton during excessive irradiance exposure. In: Dubinsky Z (ed) Photosynthesis. InTech, Rijeka, p 209–228

Laws EA (2013) Evaluation of in situ phytoplankton growth rates: a synthesis of data from varied approaches. Annu Rev Mar Sci 5:247–268

Liu H, Campbell L, Landry MR (1995) Growth and mortality rates of *Prochlorococcus* and *Synechococcus* measured with a selective inhibitor technique. Mar Ecol Prog Ser 116:277–287

Liu H, Nolla HA, Campbell L (1997) *Prochlorococcus* growth rate and contribution to primary production in the equatorial and subtropical North Pacific Ocean. Aquat Microb Ecol 12:39–47

Liu H, Campbell L, Landry MR, Nolla HA, Brown SL, Constantinou J (1998) *Prochlorococcus* and *Synechococcus* growth rates and contributions to production in the Arabian Sea during the 1995 Southwest and Northeast Monsoons. Deep Sea Res II 45:2327–2352

Llabrés M (2008) Phytoplankton cell death induced by solar ultraviolet radiation. PhD dissertation, Universitat de les Illes Balears, Palma de Mallorca

Llabrés M, Agustí S, Fernández M, Canepa A, Maurin F, Vidal F, Duarte C (2013) Impact of elevated UVB radiation on marine biota: a meta-analysis. Glob Ecol Biogeogr 22:131–144

Mackey KRM, Paytan A, Grossman AR, Bailey S (2008) A photosynthetic strategy for coping in a high-light, low-nutrient environment. Limnol Oceanogr 53:900–913

Mackey KRM, Paytan A, Caldeira K, Grossman AR, Moran D, McIlvin M, Saito MA (2013) Effect of temperature on photosynthesis and growth in marine *Synechococcus* spp. Plant Physiol 163:815–829

Madronich S, Flocke S (1997) Theoretical estimation of biologically effective UV radiation at the Earth's surface. In: Zerefos C (ed) Solar ultraviolet radiation — modeling, measurements and effects. Springer-Verlag, Berlin, p 23–48

Martín O, Peñate L, Cárdenas R, Horvath JE (2012) The photobiological regime in the very early Earth and the emergence of life. In: Seckbach J (ed) Genesis — in the beginning: precursors of life, chemical models and early biological evolution. Springer, Dordrecht, p 145–156

Mella-Flores D, Six C, Ratin M, Partensky F and others (2012) *Prochlorococcus* and *Synechococcus* have evolved different adaptive mechanisms to cope with light and UV stress. Front Microbiol 3:285

Melott AL, Thomas BC (2011) Astrophysical ionizing radiation and Earth: a brief review and census of intermittent intense sources. Astrobiology 11:343–361

Moore LR, Chisholm SW (1999) Photophysiology of the marine cyanobacterium *Prochlorococcus*: ecotypic differences among cultured isolates. Limnol Oceanogr 44: 628–638

Morel A, Ahn YH, Partensky F, Vaulot D, Claustre H (1993) *Prochlorococcus* and *Synechococcus*: a comparative study of their optical properties in relation to their size and pigmentation. J Mar Res 51:617–649

Morris JJ, Johnson ZI, Szul MJ, Keller M, Zinser ER (2011) Dependence of the cyanobacterium *Prochlorococcus* on hydrogen peroxide scavenging microbes for growth at the ocean's surface. PLOS ONE 6:e16805

Murphy CD, Roodvoets MS, Austen EJ, Dolan A, Barnett A, Campbell DA (2017) Photoinactivation of photosystem II in *Prochlorococcus* and *Synechococcus.* PLOS ONE 12: e0168991

Neale PJ (2000) Spectral weighting functions for quantifying the effects of ultraviolet radiation in marine ecosystems. In: de Mora SJ, Demers S, Vernet M (ed) The effects of UV radiation in the marine environment. Cambridge University Press, Cambridge, p 72–100

Neale PJ (2001) Modelling the effects of ultraviolet radiation on estuarine phytoplankton production: impact of variations in exposure and sensitivity to inhibition. J Photochem Photobiol B 62:1–8

Neale PJ, Thomas BC (2016) Solar irradiance changes and phytoplankton productivity in Earth's ocean following astrophysical ionizing radiation events. Astrobiology 16: 245–258

Neale PJ, Thomas BC (2017) Inhibition by ultraviolet and photosynthetically available radiation lowers model estimates of depth-integrated picophytoplankton photosynthesis: global predictions for *Prochlorococcus* and *Synechococcus*. Glob Change Biol 23:293–306

Neale PJ, Helbling EW, Zagarese HE (2003) Modulation of UVR exposure and effects by vertical mixing and advection. In: Helbling EW (ed) UV effects in aquatic organisms and ecosystems. Royal Society of Chemistry, Cambridge, p 109–134

Neale PJ, Pritchard AL, Ihnacik R (2014) UV effects on the primary productivity of picophytoplankton: biological weighting functions and exposure response curves of *Synechococcus.* Biogeosciences 11:2883–2895

Partensky F, Garczarek L (2010) *Prochlorococcus*: advantages and limits of minimalism. Annu Rev Mar Sci 2: 305–331

Partensky F, Blanchout J, Vaulot D (1999a) Differential distribution and ecology of *Prochlorococcus* and *Synechococcus* in oceanic waters: a review. Bull Inst Oceanogr 19:457–475

Partensky F, Hess WR, Vaulot D (1999b) *Prochlorococcus*, a marine photosynthetic prokaryote of global significance. Microbiol Mol Biol Rev 63:106–127

Peñate L, Martín O, Cárdenas R, Agustí S (2010) Short-term effects of gamma ray bursts on oceanic photosynthesis. Astrophys Space Sci 330:211–217

Peñate L, Cárdenas R, Agustí S (2014) The photobiological regime and the oceanic primary production. Rev Cuba Fisika 31:101–102

Piazena H, Perez-Rodrigues E, Hader DP, Lopez-Figueroa F (2002) Penetration of solar radiation into the water column of the central subtropical Atlantic Ocean-optical properties and possible biological consequences. Deep Sea Res II 49:3513–3528

Rii YM, Duhamel S, Bidigare RR, Karl DM, Repeta DJ, Church MJ (2016) Diversity and productivity of photosynthetic picoeukaryotes in biogeochemically distinct regions of the South East Pacific Ocean. Limnol Oceanogr 61:806–824

Sah JF, Krishna KB, Srivastava M, Mohanty P (1998) Effects of ultraviolet-B radiation on phycobilisomes of *Synechococcus* PCC 7942: alterations in conformation and energy transfer characteristics. Biochem Mol Biol Int 44:245–257

Shimada A, Maruyama T, Miyachi S (1996) Vertical distributions and photosynthetic action spectra of two oceanic picophytoplankters, *Prochlorococcus marinus* and *Synechococcus* sp. Mar Biol 127:15–23

Six C, Thomas JC, Brahamsha B, Lemoine Y, Partensky F (2004) Photophysiology of the marine cyanobacterium *Synechococcus* sp. WH8102, a new model organism. Aquat Microb Ecol 35:17–29

Six C, Joubin L, Partensky F, Holtzendorff J, Garczarek L (2007a) UV-induced phycobilisome dismantling in the marine picocyanobacterium *Synechococcus* sp. WH8102. Photosynth Res 92:75–86

Six C, Thomas JC, Garczarek L, Ostrowski M and others (2007b) Diversity and evolution of phycobilisomes in marine *Synechococcus* spp.: a comparative genomics study. Genome Biol 8:R259

Sobrino C, Ward ML, Neale PJ (2008) Acclimation to elevated carbon dioxide and ultraviolet radiation in the diatom *Thalassiosira pseudonana*: effects on growth, photosynthesis, and spectral sensitivity of photoinhibition. Limnol Oceanogr 53:494–505

Sommaruga R, Hofer JS, Alonso L, Gasol JM (2005) Differential sunlight sensitivity of picophytoplankton from surface Mediterranean coastal waters. Appl Environ Microbiol 71:2154–2157

Sun Z, Blanchard JL (2014) Strong genome-wide selection early in the evolution of *Prochlorococcus* resulted in a reduced genome through the loss of a large number of small effect genes. PLOS ONE 9:e88837

Tedetti M, Sempéré R (2006) Penetration of ultraviolet radiation in the marine environment: a review. Photochem Photobiol 82:389–397

Ting CS, Rocap G, King J, Chisholm SW (2002) Cyanobacterial photosynthesis in the oceans: the origins and significance of divergent light-harvesting strategies. Trends Microbiol 10:134–142

Vaulot D, Marie D, Olson R, Chisholm S (1995) Growth of *Prochlorococcus*, a photosynthetic prokaryote, in the equatorial Pacific Ocean. Science 268:1480–1482

Vincent WF, Neale PJ (2000) Mechanism of UV damage to aquatic organisms. In: de Mora SJ, Demers S, Vernet M (ed) The effects of UV radiation in the marine environment. Cambridge University Press, Cambridge, p 149–176

Vincent WF, Roy S (1993) Solar ultraviolet-B radiation and aquatic primary production: damage, protection and recovery. Environ Rev 1:1–12

Zwirglmaier K, Jardillier L, Ostrowski M, Mazard S and others (2008) Global phylogeography of marine *Synechococcus* and *Prochlorococcus* reveals a distinct partitioning of lineages among oceanic biomes. Environ Microbiol 10:147–161

Editorial responsibility: Ruben Sommaruga, Innsbruck, Austria

Submitted: March 21, 2016; Accepted: March 13, 2017
Proofs received from author(s): May 10, 2017